JACC Vol. 17, No. 6
May 1991:160B–8B

In Vivo Human Atherosclerotic Plaque Recognition by Laser-Excited Fluorescence Spectroscopy

ANTONIO L. BARTORELLI, MD, MARTIN B. LEON, MD, FACC, YARON ALMAGOR, MD, LOUIS G. PREVOSTI, MD, JULIE A. SWAIN, MD, CHARLES L. McINTOSH, MD, PhD, FACC, RICHARD F. NEVILLE, MD, MICHAEL D. HOUSE, BS, ROBERT F. BONNER, PhD

Bethesda, Maryland

Arterial wall perforation and chronic restenosis represent important factors limiting the clinical application of laser angioplasty. Discrimination of normal and atherosclerotic vessels by laser-excited fluorescence spectroscopy may offer a means of targeting plaque ablation, thereby reducing the frequency of restenosis and transmural perforation.

In this study, with use of a 325 nm low power helium-cadmium laser, in vivo endogenous surface fluorescence was excited through a flexible 200 μm optical fiber within a 0.018 in. (0.046 cm) guide wire in contact with the intima of 268 vascular interrogation sites from 48 patients either during open heart surgery or during percutaneous catheterization procedures. Fluorescence spectra could be recorded in all patients in bloodless and blood-filled arteries. Endogenous surface fluorescence was analyzed measuring peak intensity, peak position and shape index of the spectra.

Compared with normal wall, noncalcified and calcified coronary atheroma showed a 42% ($p < 0.001$) and a 58% ($p < 0.001$) decrease of peak intensity, and higher shape index ($p < 0.001$ and $p < 0.01$, respectively). In addition, peak position was shifted to longer wavelengths for noncalcified coronary atheroma ($p < 0.001$). Compared with normal aorta sites, aortic plaques demonstrated a 46% decrease of peak intensity, longer peak position wavelengths ($p < 0.05$) and a higher shape index ($p < 0.001$). Using an atheroma detection algorithm, prospective analysis of aorta and coronary spectra showed a specificity of 100% for identifying normal sites and a sensitivity of 73% for recognizing atherosclerotic sites.

This study demonstrates that in vivo laser-excited fluorescence spectroscopy of remote human arteries with optical fibers, in either a bloodless or a blood-filled environment, is feasible and accurately discriminates, with use of a real-time computer-controlled algorithm, atherosclerotic from normal vascular tissue. Thus, incorporation of fluorescence spectroscopic feedback control in a laser angioplasty system is feasible and may improve clinical results.

(J Am Coll Cardiol 1991;17:160B–8B)

The ability of laser irradiation to ablate atherosclerotic plaque was demonstrated more than 2 decades ago (1) and the feasibility of laser angioplasty was subsequently confirmed in vitro, in vivo and in early clinical trials (2–6). However, the clinical application of laser energy to achieve vascular recanalization, especially in chronic total occlusions and for definitive atheroma removal, has been limited by the high rate of vessel perforation (4,7,8) due to the inability to differentiate plaque from normal vessel wall. These limitations become even more critical in the coronary arteries, which are small in diameter, thin-walled, tortuous and frequently present structural weakness due to medial thinning in regions of plaque accumulation (9–11). Moreover, the frequency of chronic restenosis appears to be unchanged after laser angioplasty compared with that in historical control subjects treated with balloon angioplasty. Perhaps selective atheroma removal will reduce endovascular trauma and the subsequent proliferation responses that contribute to restenosis. Therefore, the goal of developing a safe and effective clinical laser angioplasty system remains elusive and the role of laser treatment in cardiovascular disease is not clearly defined.

Recently considerable attention has been focused on the technique of laser-excited fluorescence emission spectroscopy, which may allow selective targeting of laser energy to atheromatous material. This method, which has many applications in physics and biochemistry, excites target site fluorescence by means of laser irradiation and utilizes it to perform substance analysis. Previous in vitro studies (11–17) employing this technique have demonstrated its ability to discriminate normal from atherosclerotic vascular tissue in necropsy human arteries.

The purpose of this study was to assess the capability of laser-excited fluorescence emission spectroscopy to discriminate between normal and atherosclerotic human arterial vessels in vivo and to evaluate the feasibility and reliability of this technique percutaneously in blood-filled, pulsatile

From the Cardiology and Surgery Branches, National Heart, Lung, and Blood Institute, Biomedical Engineering and Instrumentation Branch Division of Research Services, National Institutes of Health, Bethesda, Maryland.

Manuscript received October 22, 1990; revised manuscript received February 5, 1991, accepted February 20, 1991.

Address for reprints: Martin B. Leon, MD, Washington Hospital Center, 110 Irving Street, N.W., Suite 4B-18, Washington, DC 20010.

0735-1097/91/$3.50

arteries. In addition, a computer algorithm capable of real-time spectra analysis for plaque discrimination was devised and prospectively evaluated.

Methods

Patient selection. Forty-eight patients, 34 men and 14 women, ranging in age from 15 to 78 years (average age 55 ± 15 years) were studied. Twenty-seven patients were examined during open heart surgery for coronary artery revascularization (n = 11), valve replacement (n = 9) or left ventricular septal myotomy-myectomy (n = 7). The remaining 21 patients were studied in the catheterization laboratory during percutaneous transluminal angioplasty of superficial femoral artery occlusion (n = 13) or during left heart diagnostic catheterization (n = 8).

The study was reviewed and approved by the Institutional Review Board of the National Institutes of Health and informed consent was obtained from all patients.

Laser-excited fluorescence emission spectroscopy. To excite fluorescence from endovascular targets, we used a system (MCM Laboratories) employing a continuous 325 nm helium-cadmium laser, coupled to a 200 μm diameter quartz core fiber within a 0.018 in. (0.046 cm) helical guide wire (MCM Laboratories). During cardiac surgery, after cardioplegic arrest, the distal tip of the fiber optic guide wire was introduced through the aortotomy or the coronary arteriotomy and hand-held in contact and perpendicular to the bloodless intimal surface. The target sites were selected by visual and tactile inspection by the operating surgeon and classified as normal, noncalcified atheroma or calcified atheroma. The noncalcified atheroma showed wide variability in thickness and color, ranging from thin, fatty streaks to thick, fibrous plaques. Only target sites identified by both the operating surgeon and a second observer as clearly representing atheroma (that is, color differences from normal vessel wall or surface changes with lumen compromise, or both) were selected for fluorescence spectroscopy.

In the catheterization laboratory, total occlusions of the superficial femoral artery and coronary arteries, detected by angiography, were chosen as abnormal sites. The fiber optic guide wire was inserted through the diagnostic catheter and advanced, under fluoroscopic control, to flush contact with the intimal surface of aortic locations in the youngest patients (37 ± 6 years) with valvular disease or hypertrophic cardiomyopathy and without angiographic evidence of coronary artery disease.

Analysis of fluorescence emission spectra. The fluorescence light emitted from the vascular tissue was acquired through the same optical fiber and focused through optical lenses into an optical multichannel analyzer (OMA, EG & G Princeton Applied Research, model 1460) composed of a diffraction-grating spectrometer, a 512 element photodiode array (detection integration time ranged from 20 to 50 ms) and a computer that analyzed, displayed and stored the spectral data curves (Fig. 1). The array detector simultaneously analyzed the fluorescence intensity over a wavelength range from 400 to 644 nm. Each spectrum was computer corrected for background radiation and, before each study, energy output from the fiber optic was determined with a power meter. Helium-cadmium laser power output ranged from 2 to 3 mW. To reduce photo-bleaching effects and blood absorption influences on tissue fluorescence spectra, which are more prominent at wavelengths <450 nm, an ultraviolet-blocking filter was used to exclude from the analysis almost all (95%) of the fluorescence wavelengths <400 nm and to partially exclude those between 400 and 450 nm.

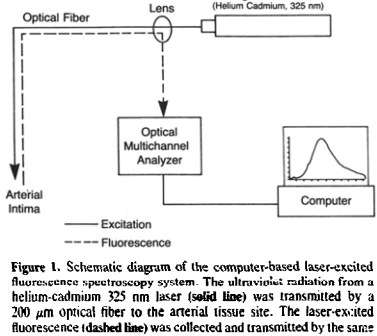

Figure 1. Schematic diagram of the computer-based laser-excited fluorescence spectroscopy system. The ultraviolet radiation from a helium-cadmium 325 nm laser (**solid line**) was transmitted by a 200 μm optical fiber to the arterial tissue site. The laser-excited fluorescence (**dashed line**) was collected and transmitted by the same optical fiber to an optical multichannel analyzer that was connected to a computer for spectra analysis and storage.

The fluorescence spectra (emission fluorescence intensity as a function of wavelength) were analyzed in real time (within 80 ms of acquisition) measuring three different variables: 1) the absolute peak intensity, which was normalized (peak intensity divided by the product of the detector exposure time and the laser power output); 2) the wavelength position, in nanometers of the fluorescence maxima, or peak position; and 3) the shape of the spectral curves. To enhance the analysis of spectra shape, each acquired spectrum was compared with a standard normal curve after equalizing peak intensity by amplification and peak position by translation (Fig. 2A and B). The standard normal curve was derived from previous in vitro and in vivo studies performed on histologically normal aorta specimens and normal aorta and coronary sites examined in the operating room (12,13).

The following formula was used to evaluate the shape of the fluorescence spectra:

$$SI = \frac{[(\Delta 1)^2 + (\Delta 2)^2 + (\Delta 3)^2 + (\Delta 4)^2 + (\Delta 5)^2]}{5} \times 100.$$

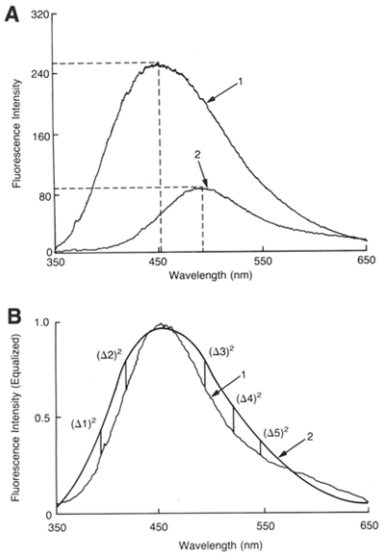

Figure 2. A, Representative fluorescence emission spectra from a normal coronary site **(1)** and a noncalcified coronary atheroma **(2).** The fluorescence spectra were analyzed measuring three different variables: 1) normalized absolute fluorescence peak intensity (absolute peak intensity/detector exposure time × laser power output); 2) wavelength position of the fluorescence maxima or peak position; and 3) shape of the curve. **B,** The shape of each acquired spectrum **[1]** was compared with the shape of a standard normal curve **[2]** by equalizing peak intensity by amplification and peak position by translation. A formula utilizing the sum of five least square residuals of fluorescence intensity, here indicated by $(\Delta)^2$, computed at different wavelength positions (see text), was used to generate a numeric index, the shape index that expressed the shape difference between the acquired spectrum and the standard normal curve.

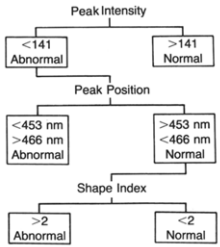

Figure 3. Flow diagram of the atheroma detection algorithm. The threshold values for peak intensity, peak position and shape index and the sequence used by the algorithm for the analysis of the fluorescence spectra are shown. Diagnosis of atherosclerotic plaque was made when peak intensity was abnormal and either peak position or shape index were also abnormal. Conversely, normal sites were diagnosed when they showed either normal peak intensity or both normal peak position and normal shape index.

where SI is shape index and $(\Delta_n)^2$ represents least square residuals computed at different wavelength positions. The wavelength positions for the least square residuals calculation were selected at five fixed points relative to the peak position of each spectrum; −42, −36, +52, +83 and +114 nm. These fixed wavelength positions were chosen to optimize the shape differences between normal and abnormal spectra after visual assessment of the data set. This formula was used to generate the shape index, a numeric index that expressed the shape changes between the acquired spectra and the standard normal curve (Fig. 2B). As the shape of the spectra became more normal the shape index value (that is, the sum of the least square residuals obtained by comparison with the standard normal curve) decreased and, conversely, the shape index increased when the shape became more abnormal. At each site five consecutive spectra were recorded at 120 ms intervals to examine intrasite variability. Peak intensity, peak position and shape index values were obtained from the average of these five consecutive spectra.

Atheroma detection algorithm. The fluorescence spectra obtained in the operating room from aorta and coronary sites of the first 20 consecutive patients (Group A) were analyzed to determine peak intensity, peak position and shape index values. From these data, to maximize the specificity of normal site recognition while maintaining high sensitivity for atheroma detection, we assigned algorithm cutoff values as follows: peak intensity <141, peak position <453 or >466 nm and shape index >2. Because of individual data overlap (see Results) a multistate algorithm (Fig. 3) was used to discriminate plaque from normal sites. Diagnosis of atherosclerotic plaque was made when peak intensity was abnormal and either peak position or shape index was also abnormal. Conversely, normal sites were diagnosed when they showed either normal peak intensity or both normal peak position and normal shape index.

Subsequently, the algorithm was prospectively tested in 7 patients in the operating room (Group B1) during probing of normal aorta (n = 19) and coronary sites (n = 6), and in 21 patients in the catheterization laboratory (Group B2) during probing of the superficial femoral artery (n = 59) and coronary artery (n = 8) total occlusion sites and normal aortic sites (n = 33).

Statistical analysis. Comparison of the spectra variable values was made with unpaired Student's *t* test analysis.

Table 1. Number, Location and Characteristics of the Examined Arterial Sites in All Patients (n = 48)

	Aorta		Coronary Arteries		SFA
	OR	CL	OR	CL	CL
Total examined sites	63	33	57	8	59
Normal sites	84	33	35	—	—
Noncalcified plaque	12	—	15	—	—
Calcified plaque	—	—	7	—	—
Total occlusion	—	—	—	8	59

CL = catheterization laboratory; OR = operating room; SFA = superficial femoral artery.

Statistical significance was accepted at the level of $p < 0.05$. All grouped data are reported as mean values ± 1 SD.

The inter-site variability of fluorescence spectra was evaluated in 16 patients by determining the standard deviation of peak intensity, peak position and shape index values obtained in 52 normal aorta sites in a bloodless field (n = 19) and in a blood-filled field (n = 33). Each variable value was obtained from the average of five consecutive spectra for each site. The intrasite variability was examined in five patients by determining the mean of the standard deviations of peak intensity, peak position and shape index values obtained from the individual spectra of 22 blood-filled normal aorta sites.

Results

Vascular interrogation sites (Table 1). Adequate emission fluorescence spectra were obtained from all interrogation sites in all 48 patients in both bloodless (operating room) and blood-filled (catheterization laboratory) arteries. In the operating room there were 315 recorded spectra from 63 aortic sites and 285 spectra from 57 coronary artery sites. Seven of the 22 abnormal coronary sites were calcified, whereas none of the 12 aortic lesions showed evidence of calcification (Table 1). In the catheterization laboratory, 500 spectra were obtained from 59 superficial femoral artery proximal occlusion sites, 8 coronary proximal occlusion sites and 33 normal aortic sites (Table 1).

Laser-excited fluorescence spectroscopy (Table 2). The mean values of peak intensity, peak position and shape index of normal and atherosclerotic coronary artery and aortic locations obtained from the first 20 consecutive patients studied in the operating room (Group A) are summarized in Table 2. The laser-excited fluorescence spectra acquired from normal aortic and coronary sites showed comparable spectral morphology with similar peak position and shape index values (Fig. 4 and 5). It is noteworthy, however, that the mean value of peak intensity in aortic sites was 58% higher ($p < 0.001$) than that from coronary arteries.

Compared with normal sites, noncalcified and calcified coronary atheroma showed 1) lower values of fluorescence peak intensity, 42% for noncalcified plaque ($p < 0.001$) and 58% for calcified plaque ($p < 0.001$); 2) fluorescence peak position shifted to longer wavelengths for noncalcified plaque ($p < 0.001$) or shorter wavelengths for calcified plaque ($p < 0.001$); and 3) higher shape index for both noncalcified ($p < 0.001$) and calcified plaque ($p < 0.01$) (Fig. 4). Aortic plaques and normal aortic sites exhibited spectral differences comparable with those observed among coronary arteries (Fig. 5). Compared with normal aortic sites, aortic plaques were characterized by a 46% decrease of the fluorescence peak intensity ($p < 0.001$), a longer fluorescence peak position ($p < 0.05$) and a fourfold increase of the shape index ($p < 0.001$) (Fig. 5).

Despite these statistically significant changes of the three spectral variables associated with atherosclerotic plaque in both aortic and coronary artery regions, there was a considerable overlap of the individual values. Therefore, the sensitivity and specificity of atheroma detection by fluorescence spectroscopy utilizing any or all of the individual variables were unacceptable, prompting the development of the aforementioned multistage algorithm.

Atheroma detection algorithm (Table 3). Initially the algorithm with assigned cutoff values was retrospectively applied to the spectra of the first 20 consecutive patients (Group A). It correctly diagnosed all normal coronary artery sites and all but two calcified coronary atheroma (Fig. 6). Among the aortic sites, the algorithm diagnosis was correct in all normal sites and all but four abnormal sites (Fig. 7).

To evaluate prospectively the sensitivity and specificity of the algorithm, we studied 28 additional patients (Groups B1 and B2). The mean values of peak intensity, peak position and shape index obtained in these patients are shown in

Table 2. Mean Values of Normalized Intensity, Peak Position and Shape Index of Aortic and Coronary Artery Sites in the First 20 Consecutive Patients Studied in the Operating Room (Group A)

	Normal Aorta	Aortic Plaque	Normal Coronary Artery	Coronary Plaque	Calcified Coronary Plaque
PI	216 ± 50	117 ± 54*	137 ± 49‡	79 ± 28§	58 ± 31§
PP	463 ± 3	467 ± 4†	462 ± 2	466 ± 48	456 ± 8§
SI	0.8 ± 0.6	4.1 ± 4.1*	0.7 ± 0.8	6.7 ± 3.7§	2.2 ± 1.9†

Values are mean values ± 1 SD. *$p < 0.001$ versus normal; †$p < 0.05$ versus normal; ‡$p < 0.001$ versus normal aorta. PI = peak intensity; PP = peak position; SI = shape index.

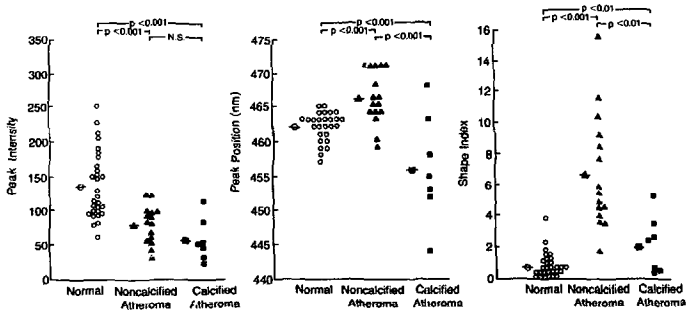

Figure 4. Individual values of peak intensity, peak position and shape index of the spectra of 51 coronary artery sites from 10 patients of Group A. **Open circles** represent normal sites, **solid triangles** noncalcified atheroma and **solid squares** calcified atheroma. The mean values of the three variables for each category are also shown.

Figure 5. Individual values of peak intensity, peak position and shape index of the spectra of 44 aortic sites from 11 patients of Group A. **Open circles** represent normal sites and **solid triangles** noncalcified atheroma. The mean values of the three variables for each site category are indicated by **larger symbols with bars.**

Table 3. The sensitivity of atheroma recognition in blood-filled superficial femoral artery and coronary proximal occlusion sites (n = 67) was, respectively, 71% and 88% (average 73%). The specificity for normal site detection in both blood-filled and bloodless aorta sites (n = 58) was 100%.

Fluorescence spectra variability (Tables 2 and 3). The mean values of the spectral variables and their standard deviations were similar for normal aorta in the retrospective Group A (operating room) patients and the prospective patients in Groups B1 (operating room) and B2 (catheterization laboratory). The specificity of normal site recognition

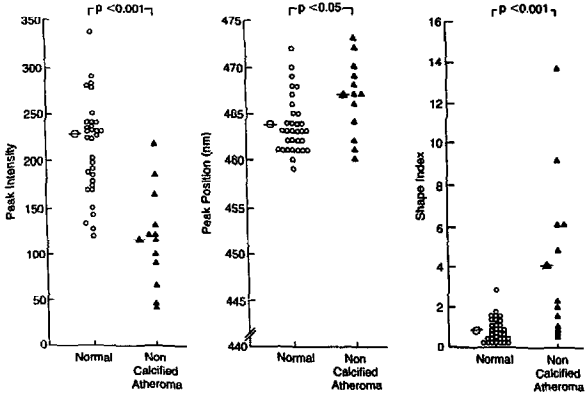

Table 3. Mean Values of Spectral Variables of Aorta, Coronary Arteries and Superficial Femoral Artery in the Patients of Groups B1 and B2 (n = 12)

	Operating Room			Catheterization Laboratory		
	PI	PP	SI	PI	PP	SI
Normal aorta	241 ± 78	462 ± 2	0.6 ± 0.5	218 ± 63	462 ± 2	0.3 ± 0.3
Normal coronary artery	168 ± 39	463 ± 1	0.9 ± 1.0	—	—	—
SFA occlusion	—	—	—	99 ± 46	471 ± 5	2.6 ± 4.1
Coronary occlusion	—	—	—	47 ± 52	479 ± 6	3.0 ± 3.0

Abbreviations as in Tables 1 and 2.

was unchanged when the algorithm was applied to bloodless (Groups A and B1) and blood-filled sites (Group B2).

The analysis of individual sequential spectra from the same tissue site did not significantly increase errors in estimation of normal site variable values in the 22 aortic sites from five patients studied in the catheterization laboratory. Here, the mean intrasite variability of the variables (peak intensity ± 10, peak position ± 1.4 and shape index ± 0.25) for individual spectra was significantly less than the inter-site variability (peak intensity + 69, peak position + 2.0, shape index + 0.42) for averaged spectra at all 52 sites in Groups B1 and B2.

Discussion

The arterial wall of normal and atherosclerotic vessels exhibits natural fluorescence when irradiated by ultraviolet light at wavelengths of 300 to 400 nm. Previous work has confirmed the presence of endogenous fluorophore substances in the arterial wall as well as in the atheromatous plaque. Most of the fluorescence of the normal arterial wall is thought to originate from elastin and collagen components (14).

Changes in fluorescence patterns at the site of atherosclerotic lesions. This has been related to changes in the concentration of collagen and elastin, as well as the presence of specific fluorophores, such as flavoproteins and carotenoids (18–21). These findings have raised interest in laser-excited fluorescence spectroscopy as a diagnostic tool to obtain meaningful information about the composition of arterial tissue and to direct laser ablation of arterial obstructions. Since the initial observation of Kittrell et al. (22), other studies have demonstrated that the spectral features of normal arteries at necropsy differ from those of atherosclerotic plaques (23–26). In addition, evidence has been accumulated showing that, after plaque ablation, the fluorescence spectra revert to a normal pattern (12,25). This is to be expected because the media layer is not generally affected by

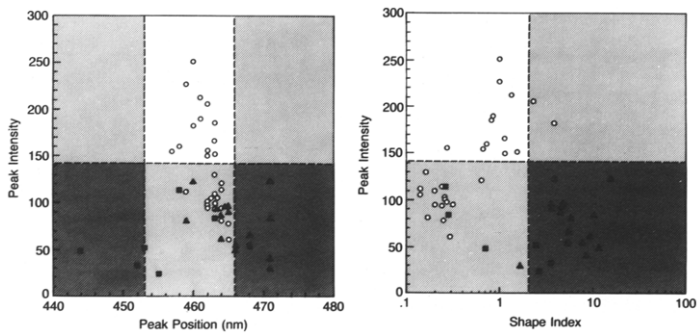

Figure 6. Graphic representation of the atheroma detection algorithm applied to 51 coronary artery sites from 10 patients of Group A. **Open circles** represent normal sites, **solid triangles** noncalcified atheroma and **solid squares** calcified atheroma. Peak intensity is plotted against peak position (**left plot**) and against shape index (**right plot**, note semilogarithmic scale). To recognize a site as atheroma (**dark shaded areas**), the algorithm required abnormal peak intensity and peak position (**left plot**) or abnormal peak intensity and shape index (**right plot**). Light-shaded areas of both plots designate sites with one abnormal and one normal variable. **Nonshaded areas** have two normal variables. Using threshold values of <141 for peak intensity, <453 or >466 nm for peak position and >2 for shape index, all normal sites and all but two calcified atheroma sites were correctly diagnosed.

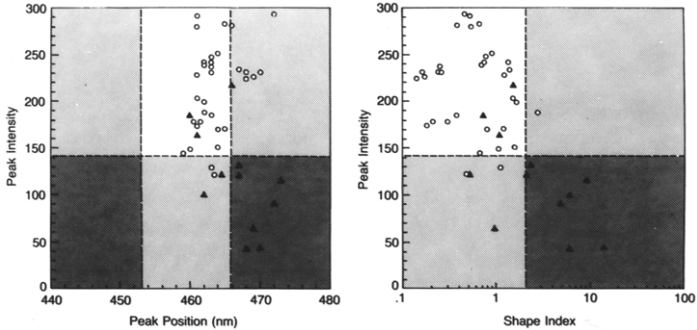

Figure 7. Graphic representation of the atheroma detection algorithm applied to 44 aorta sites from 11 patients of Group A. **Open circles** represent normal sites and **solid triangles** noncalcified atheroma. Peak intensity is plotted against peak position (**left plot**) and against shape index (**right plot**, note semilogarithmic scale). The threshold values and the area designations are the same as in Figure 6. The algorithm correctly diagnosed all normal sites and all but four abnormal sites.

atherosclerosis and exhibits spectroscopic characteristics that are strikingly similar to those of the healthy intimal surface (26,27).

These studies have prompted the concept of a "smart" laser angioplasty system that incorporates low power laser irradiation for diagnostic fluorescence spectroscopy to guide delivery of high power laser irradiation for plaque ablation. In such a system a fluorescence spectrum of the normal media underlying plaque could inhibit the high power ablative pulse and guide repositioning of the fiber tip to the desired target. However, to establish the feasibility of a spectroscopic feedback mechanism to guide laser angioplasty in a clinical setting, it is fundamental to confirm that the diagnostic capability demonstrated in cadaver arterial wall is maintained in living tissue. Moreover, to use fluorescence signals for feedback control, one must have the means of analyzing the data in real time to permit the automated and simultaneous control of selective plaque ablation by laser energy. Finally, to be implemented in a laser angioplasty system, this technique has to demonstrate its ability to collect reliable fluorescence spectra in living blood-filled arteries where vessel motion and blood interference are serious obstacles to consistent tissue contact.

Autofluorescence in normal artery wall from plaque. In this study autofluorescence was excited in the aorta and coronary arteries of patients using a low power helium-cadmium laser at 325 nm. Utilizing a common optical pathway, after tissue absorption of the transmitting laser light, resultant fluorescence light from the artery wall was captured by the flexible fiber optic guide wire and analyzed by standard computer-controlled techniques. A main goal of the study was to develop an algorithm based on fluorescence spectra characteristics that could differentiate plaque from normal arterial wall with high sensitivity and specificity. In the present study the diagnostic sequence, including fluorescence spectra analysis, was performed within 80 ms, thus having the capability of real time integration with a pulsed treatment laser for tissue ablation.

In both normal aortic and normal coronary artery specimens, the fluorescence spectra appeared strikingly reproducible even though collected from distinct anatomic locations in different patients. Furthermore, studies conducted in the catheterization laboratory indicated that, despite catheter immersion in a blood-filled intravascular field, the remote acquisition of fluorescence spectra was possible and showed no significant differences with the corresponding spectra collected in bloodless vessels. Direct contact with the intimal surface of the vessel was easily achieved by light anterograde force applied to the fiber optic guide wire that insured flush tissue contact, displacing the intervening blood zone.

Compared with normal arterial sites, both coronary and aortic atherosclerotic sites demonstrated a reduction in fluorescence peak intensity associated with higher shape indices. In addition, the fluorescence peak position of atheroma occurred at longer wavelengths or, in the case of calcified coronary sites, at shorter wavelengths. An interesting finding in normal vessels was the significantly lower fluorescence peak intensity exhibited by coronary arteries compared with aorta. This difference in autofluorescence might be related to the different structural composition of the media of these arteries. Aorta media contains many layers of elastin-rich fibers with strong fluorescence, whereas coronary artery media consists mainly of smooth muscle cells with less interspersed elastin.

Blood-filled versus bloodless arterial sites. In the initial study, to retrospectively analyze in vivo fluorescence spectra for future algorithm development, averages of five spectra at each site were obtained from 20 patients in bloodless aortic and coronary artery locations during cardiac surgery. Thereafter, to simulate the situation of guiding laser ablation percutaneously, the algorithm was prospectively applied in 28 patients to the analysis of spectra from superficial femoral artery and coronary proximal occlusions (both presumed to be abnormal) and aortic sites in young patients without coronary artery disease (presumed to be normal).

Fluorescence spectroscopy showed no statistically significant difference of the mean values of peak intensity and peak position between the blood-filled aortic sites examined in the catheterization laboratory and all the sites examined in the operating room under visual inspection (225 ± 62 vs. 218 ± 63 and 463 ± 3 vs. 462 ± 2 nm, respectively). In addition, the shape index value was even lower and showed less variability in the blood-filled sites than in the bloodless sites (0.69 ± 0.55 vs. 0.33 ± 0.34), indicating that they were nearly identical to the standard normal curve and that blood and vessel motion did not decrease the ability to acquire reliable spectra.

The spectra were collected and analyzed at a speed sufficient to guide laser ablation at repetition rates of up to five laser pulses per second. Although the sensitivity of atheroma recognition in blood-filled superficial femoral artery and coronary proximal occlusion sites was <100% (71% and 88%, respectively), the specificity for normal site detection in both blood-filled and bloodless aortic sites was 100%. This is to be expected because the atheroma detection algorithm was devised to maximize the specificity of normal tissue recognition, so that reduction in sensitivity could also be related to the heterogeneous composition of atheromatous tissue compared with normal vascular tissue.

The variability of the spectral variables obtained from a single interrogation site reflects variations in the concentration of fluorescent and absorbing molecules in normal and abnormal tissues after repetitive laser exposure, intrinsic instrument variability factors and varying fiber to tissue contact. In this study the mean values of the spectral variables of normal sites obtained percutaneously in a blood-filled environment were equivalent to those obtained in a bloodless field during surgery (Table 3). The individual spectra were obtained every 200 ms over a cardiac cycle that maximizes the potential variability in spectral variable values due to blood flow and heart motion. At a given site, the variability of spectral variables over the cardiac cycle was less than the inter-site variability of peak intensity, peak position and shape index values in either a blood-filled or a bloodless field. Thus, the feasibility of fluorescence spectroscopic guidance was not diminished by relying on individual spectra obtained in a blood field.

Fluorescence spectra of both the healthy and the atherosclerotic arterial wall are susceptible to changes when exposed to laser radiation. These photobleaching changes, which are more pronounced for shorter ultraviolet wavelength components, tend to diminish the difference between normal and abnormal tissue spectra and thus may play an important role when laser ablation and fluorescence spectroscopy are employed simultaneously.

Future directions. In this study a small diameter optical fiber was used to deliver the laser light and to collect the return fluorescence. The possibility of incorporating spectroscopic guidance into more practical multifiber catheter delivery systems raises new issues, such as uniform and adequate contact between a larger catheter tip and the plaque surface in a blood field and the interpretation of spectra obtained from a large heterogenous tissue area. Recognition of specific plaque subtypes (fibrous, fatty, calcific or thrombotic) might improve efficacy of plaque ablation during laser angioplasty. Laser dosimetry might be adjusted for specific lesion composition to minimize the risk of perforation and improve recanalization efficacy. Therefore, further studies on multifiber laser catheters, as well as improved algorithms for plaque subtype discrimination using laser-excited fluorescence spectroscopy, are needed.

Conclusions. The present study demonstrates that real-time acquisition and analysis of fluorescent spectra in vivo from human vascular tissue are feasible and can discriminate with high specificity and sensitivity normal from atheromatous vascular tissue. Moreover, it showed that laser-excited fluorescence emission spectroscopy can be successfully performed percutaneously and that reliable fluorescence spectra can be collected in blood-filled arteries despite vessel motion and pulsatile flow. Finally, the fact that the analysis was performed in real time demonstrated that it can be used to guide simultaneous laser ablation at repetition rates of up to 5 pulses/s. Thus, real-time fluorescence-guided laser angioplasty has the potential to achieve selective atheroma ablation that may prevent transmural perforations while also limiting vessel wall injury, thereby reducing the frequency of restenosis.

References

1. McGuff PE, Bushnell D, Soroff HS, Deterling RA. Studies of the surgical applications of laser (light amplification by stimulated emission of radiation). Surg Forum 1963;14:143–5.
2. Grundfest WS, Litvack F, Forrester JS, et al. Laser ablation of human atherosclerotic plaque without adjacent tissue injury. J Am Coll Cardiol 1985;5:929–33.
3. Abela GS, Seeger JM, Barbieri E, et al. Laser angioplasty with angioscopic guidance in humans. J Am Coll Cardiol 1986;8:184–92.
4. Choy DSJ, Stertzer SH, Myler RD, Marco J, Fournay G. Human coronary laser recanalization. Clin Cardiol 1984;7:377–81.
5. Ginsberg R, Wexler L, Mitchell RS, Profitt D. Percutaneous transluminal laser angioplasty for treatment of peripheral vascular disease: clinical experience with 16 patients. Radiology 1985;156:619–24.
6. Abela GS, Normann SJ, Cohen DM, et al. Laser recanalization of occluded atherosclerotic arteries in vivo and in vitro. Circulation 1985; 71:403–11.
7. Nordstrom LA, Castaneda-Zuniga WR, Young EG, Seggern KB. Direct argon laser exposure for recanalization of peripheral arteries: early results. Radiology 1988;168:359–64.

8. Isner JM, Donaldson RF, Funai JT, et al. Factors contributing to perforations resulting from laser coronary angioplasty: observations in an intact human postmortem preparation of intraoperative laser coronary angioplasty. Circulation 1985;72(suppl II):II-191–9.
9. Hartman JD. Structural changes within the media of coronary arteries related to intimal thickening. Am J Pathol 1977;89:13–34.
10. Almagor Y, Leon MB, Bartorelli AL, et al. Media thinning of severely diseased coronary arteries: guidelines for new interventional procedures (abstr). J Am Coll Cardiol 1989;13:194A.
11. Isner JM, Donaldson RF, Fortin AH, Tischler A, Clarke RH. Attenuation of the media of coronary arteries in advanced atherosclerosis. Am J Cardiol 1986;58:937–9.
12. Leon MB, Lu DY, Prevosti LG, et al. Human arterial surface fluorescence: atherosclerotic plaque identification and effects of laser atheroma ablation. J Am Coll Cardiol 1988;12:94–102.
13. Bartorelli AL, Almagor Y, Prevosti LG, et al. In vivo coronary plaque recognition by laser-induced fluorescence spectroscopy (abstr). Circulation 1988;78(suppl II):II-294.
14. Macfarlane TWR, Petrowski S, Rigutto L, Roach MR. Computer-based video analysis of cerebral arterial geometry using the natural fluorescence of the arterial wall and contrast enhancement techniques. Blood Vessels 1983;20:161–71.
15. Banga I, Bihari-Varga M. Investigations of free and elastin-bound fluorescent substances present in the atherosclerotic lipid and calcium plaques. Connect Tissue Res 1974;2:237–41.
16. Tinker DH, Rucker RB, Tappel AL. Variation of elastin fluorescence with method of preparation: determination of the major fluorophore of fibrillar elastin. Connect Tissue Res 1983;2:299–308.
17. Blomfield J, Farrar JF. Fluorescence spectra of arterial elastin. Biochem Biophys Res Commun 1967;28:346–51.
18. Blankenhorn DH, Braunstein H. Carotenoids in man. III. The microscopic pattern of fluorescence in atheroma and its relation to their growth. J Clin Invest 1958;37:160–5.
19. Blankenhorn DH, Freiman DG, Knowles HC. Carotenoids in man. The distribution of epiphasic carotenoids in atherosclerotic lesions. J Clin Invest 1956;35:1243–7.
20. Prince MR, Deutsch TF, Mathews-Roth MM, Margolis R, Parrish JA, Oseroff AR. Preferential light absorption in atheromas in vitro: implication for laser angioplasty. J Clin Invest 1986;78:295–302.
21. Benson RC, Meyer RA, Zaruba ME, McKhann GM. Cellular autofluorescence: is it due to flavins? J Histochem Cytochem 1978;27:44–8.
22. Kittrell C, Willett RL, de los Santos-Pacheo C, et al. Diagnosis of fibrous arterial atherosclerosis using fluorescence. Appl Opt 1985;24:2280–1.
23. Deckelbaum LI, Lam JK, Cabin HS, Clubb KS, Long MB. Discrimination of normal and atherosclerotic aorta by laser-induced fluorescence. Lasers Surg Med 1987;7:330–5.
24. Sartori M, Weilbaecher D, Valderrama GL, et al. Laser-induced autofluorescence of human arteries. Circ Res 1988;63:1053–9.
25. Laufer G, Wollenek G, Hohla K, et al. Excimer laser-induced simultaneous ablation and spectral identification of normal and atherosclerotic arterial tissue layers. Circulation 1988;78:1031–9.
26. Richards-Kortum RR, Matha A, Kolubayev T, et al. Spectroscopic diagnosis for control of laser treatment of atherosclerosis. In: Svanberg S, Person W, eds. Laser Spectroscopy VIII. Proceedings of the Eighth International Conference on Laser Spectroscopy. Berlin: Springer-Verlag, 1987;366–9.
27. Bartorelli AL, Bonner R, Almagor Y, et al. Enhanced recognition of plaque composition in vivo using laser-excited fluorescence spectroscopy (abstr). J Am Coll Cardiol 1989;13:54A.